JOURNAL OF GEOPHYSICAL RESEARCH, VOL. 113, B05302, doi:10.1029/2007JB005277, 2008

Potential for earthquake triggering from transient deformations

Heather M. Savage[1,2] and Chris Marone[1]

Received 19 July 2007; revised 29 November 2007; accepted 8 January 2008; published 2 May 2008.

[1] We report on laboratory experiments in which stick-slipping shear surfaces are subject to transient stressing to simulate earthquake triggering by seismic waves. Granular layers and bare granite surfaces were sheared in a servo-controlled deformation apparatus in double-direct shear. The seismic waves from an earthquake and tectonic load were simulated by superimposing a loading rate sinusoid on a constant shear loading rate. The dependence of triggered stick-slip failure on fault stress state and architecture was analyzed. Fault architecture was evaluated by varying gouge layer thickness (2–6 mm) and studying bare granite surfaces. We compare the shortened recurrence times for faults under transient loading conditions to the consistent recurrence intervals under constant loading rate. Our results imply that triggering depends on oscillation amplitude and frequency, as well as properties of the fault. Larger-amplitude dynamic stresses reduce stick-slip recurrence intervals for granular layers, whereas failure times for granite surfaces are uncorrelated with oscillation amplitude. Granular layers have shorter recurrence rates at higher frequency, whereas the recurrence intervals of granite surfaces are lengthened or unaffected by high-frequency oscillations. Higher frequencies can inhibit failure when fault slip exceeds a critical distance, D_c, prior to peak velocity and encourages failure if D_c is achieved postpeak velocity. Increasing velocity temporarily strengthens faults, whereas velocity reduction further weakens and promotes failure, as predicted by the rate-and-state friction laws. Our results may explain variations in earthquake triggering thresholds and imply that high-frequency thresholds may not be constant, as has been previously proposed.

Citation: Savage, H. M., and C. Marone (2008), Potential for earthquake triggering from transient deformations, *J. Geophys. Res.*, *113*, B05302, doi:10.1029/2007JB005277.

1. Introduction

[2] Earthquake triggering from the passage of seismic waves has been shown to be a ubiquitous process, occurring in both the far field [*Hill et al.*, 1993; *Stein*, 1999; *Kilb et al.*, 2000; *Gomberg et al.*, 2001; *Husen et al.*, 2004b; *Prejean et al.*, 2004; *West et al.*, 2005] as well as close to the source of the triggering event [*Gomberg et al.*, 2003; *Felzer and Brodsky*, 2006]. Dynamic triggering can occur as the wave train passes [*Gomberg et al.*, 2004], or for days and weeks after the triggering event [*Brodsky*, 2006]. Earthquakes can be triggered at active plate boundaries or in seismically stable environments [*Hough et al.*, 2003; *Gomberg et al.*, 2004].

[3] Despite well-documented occurrence of earthquake triggering, our understanding of triggering thresholds is incomplete. The maximum amplitude of the seismic waves has been proposed as a likely threshold for triggering [*Gomberg and Johnson*, 2005; *Johnson and Jia*, 2005]. *Gomberg et al.* [2004] demonstrated that earthquake triggering from the Denali earthquake followed the direction of rupture and therefore the path with greatest wave amplitude. However, if a seismic wave amplitude threshold exists, it varies between faults [*Brodsky et al.*, 2000; *Gomberg and Davis*, 1996]. Indeed, *Harrington and Brodsky* [2006] found that earthquakes were not triggered in Japan by seismic waves with amplitudes similar to triggering events elsewhere. An alternate hypothesis is that frequency of the triggering event affects the threshold. One study of triggered seismicity at Long Valley Caldera found that triggering required low-frequency energy [*Brodsky and Prejean*, 2005]; however, others indicate that high frequencies are more likely to trigger seismicity [*Gomberg and Davis*, 1996].

[4] Existing field observations and friction theory indicate that triggering almost certainly depends on a fault's stress state, i.e., how close the fault is to failure when the transient deformation occurs, which in turn depends on the time since the last major earthquake on that fault and the tectonic loading rate. Once a fault fails in an earthquake, healing or strengthening processes begin while at the same time slowly applied tectonic forces stress the fault. As it is stressed, the nature of the fault zone also evolves, but eventually the accumulating stresses and creep strain will again produce the failure condition and an earthquake

[1] Rock Mechanics Laboratory, Department of Geosciences, Pennsylvania State University, University Park, Pennsylvania, USA.
[2] Now at the Earth and Marine Science Department, University of California, Santa Cruz, California, USA.

0148-0227/08/2007JB005277$09.00

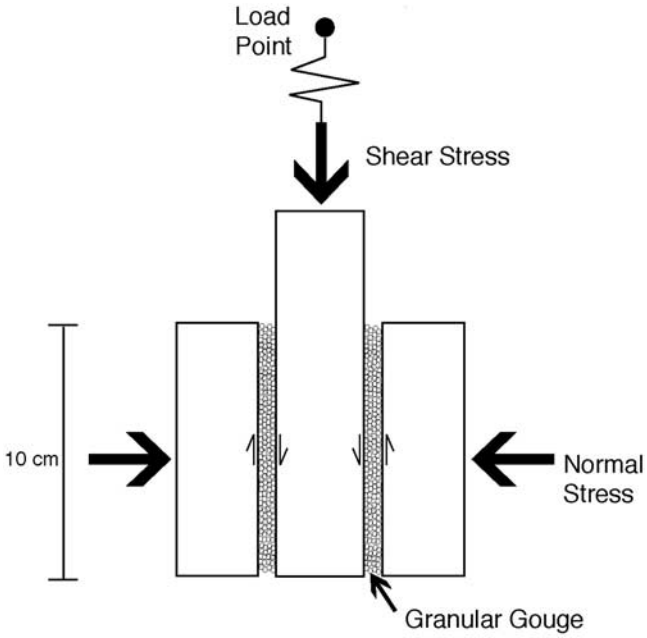

Figure 1. Diagram of double-direct shear configuration showing granular gouge layers between the three block configurations. Experiments on bare granite surfaces used granite forcing blocks. A constant normal stress was applied during shearing in all experiments.

recurs. Although studies have shown that faults are more likely to be dynamically triggered when the fault is closer to failure (i.e., has been stressed by tectonic loading for a longer time) [*Gomberg et al.*, 1997], this does not imply that the transient stresses have simply caused the fault to reach its failure strength; instead the failure strength is altered by the change in stressing rate associated with the seismic wave. Faults may not be susceptible to dynamic triggers unless the fault has reached a state of critical stress in its interseismic period.

[5] In addition to properties of the seismic wave and fault state, fault zone architecture (i.e., fault zone width, roughness, and properties of the fault gouge) may influence a fault's susceptibility to dynamic triggering. Faults whose frictional strength is controlled by a gouge layer may react differently to dynamic stresses than a fault without a significant gouge layer. *Marone and Scholz* [1988] found that the upper stability limit of crustal faults depends on whether a thick gouge layer is present; faults without a significant gouge layer are capable of nucleating earthquakes at shallower depths. In laboratory experiments, the generation of a gouge layer with progressive slip has a stabilizing effect, tending to inhibit stick slip [*Engelder et al.*, 1975; *Byerlee and Summers*, 1976; *Wong and Zhao*, 1990]. One of the purposes of this study is to investigate whether fault zone architectures have a similar stabilizing effect in relation to transient triggers.

[6] Our experiments are conducted on laboratory faults experiencing violent stick-slip behavior analogous to the earthquake cycle [*Brace and Byerlee*, 1966]. We explore aspects of earthquake triggering such as dependency on fault zone architecture, stress state with respect to the seismic cycle, and properties of the seismic wave by superimposing bursts of oscillating shear velocity on a constant background loading rate. Sinusoids of different amplitude, frequency and duration were used to simulate a range of triggerring event sizes. To recreate fault zones of differing maturity, we shear gouge layers of different thicknesses ranging from 0 (bare granite surfaces) to 6 mm.

2. Experimental Procedure

[7] Experiments were conducted in a servo-controlled biaxial deformation apparatus with a double-direct shear configuration (Figure 1). For experiments with synthetic gouge, layers of glass beads were sheared between $10 \times 10 \times 2$ cm side steel blocks and a center block $10 \times 15 \times 3$ cm so that a constant nominal contact area of 10×10 cm was maintained throughout shear. The forcing blocks have triangular grooves 0.8 mm deep and 1 mm in wavelength perpendicular to the shear direction. These grooves force shear to occur within the layer instead of along the boundary. The samples were loaded in controlled shear displacement with 0.1 μm resolution and at constant normal stress of 5 MPa (with 0.1 kN resolution). This normal stress is high enough for stresses at contact junctions to reach the inelastic yield point and to activate physicochemical processes that govern time-dependent and rate/state friction effects, yet low enough to eliminate grain comminution and the resulting variations in frictional behavior with net fault offset. The stiffness of the vertical load frame is 5 MN/cm or 250 MPa/cm when expressed as the shear stress on a double direct shear sample with nominal friction contact dimensions of 10 cm $\times$ 10 cm. The load point velocity history consisted of a linear function with a sinusoid sporadically superimposed to mimic a tectonic load and seismic waves, respectively (Figure 2). The background loading rate was held constant at 5 μm/s. The amplitude, frequency and duration of the triggering stress were varied to assess triggering thresholds (Table 1). The displacement control was updated at a rate of 300 Hz and the output signal was recorded at 100 Hz.

[8] We conducted experiments on both Westerly granite and soda lime glass beads (size distribution 105–149 μm, Mo-Sci Corporation, Rolla, Missouri). Glass beads have material properties similar to quartz and are ideal for these tests due to the repeatability of the magnitude and recurrence interval of stick-slip events. Steel guide plates and tape were attached to the unconfined sides of the sample configuration to hold the blocks together until loaded. Copper shims were attached at the bottom of the sample layers to minimize gouge loss. A latex rubber sheet of 0.01″ thickness was taped over the copper shims, to minimize avalanching along the unconfined edges of the layers. For experiments with granite, we created a double-direct shear configuration with one center block and two side blocks composed of Westerly granite, again with nominal contact area of 10×10 cm throughout the experiment. We investigated the role of surface roughness. Initially, the surfaces were surface ground flat and finished with #60-grit polish, which produces $\sim$100 μm RMS roughness (rough granite experiment – p936). We evaluated changes in behavior as surfaces were progressively

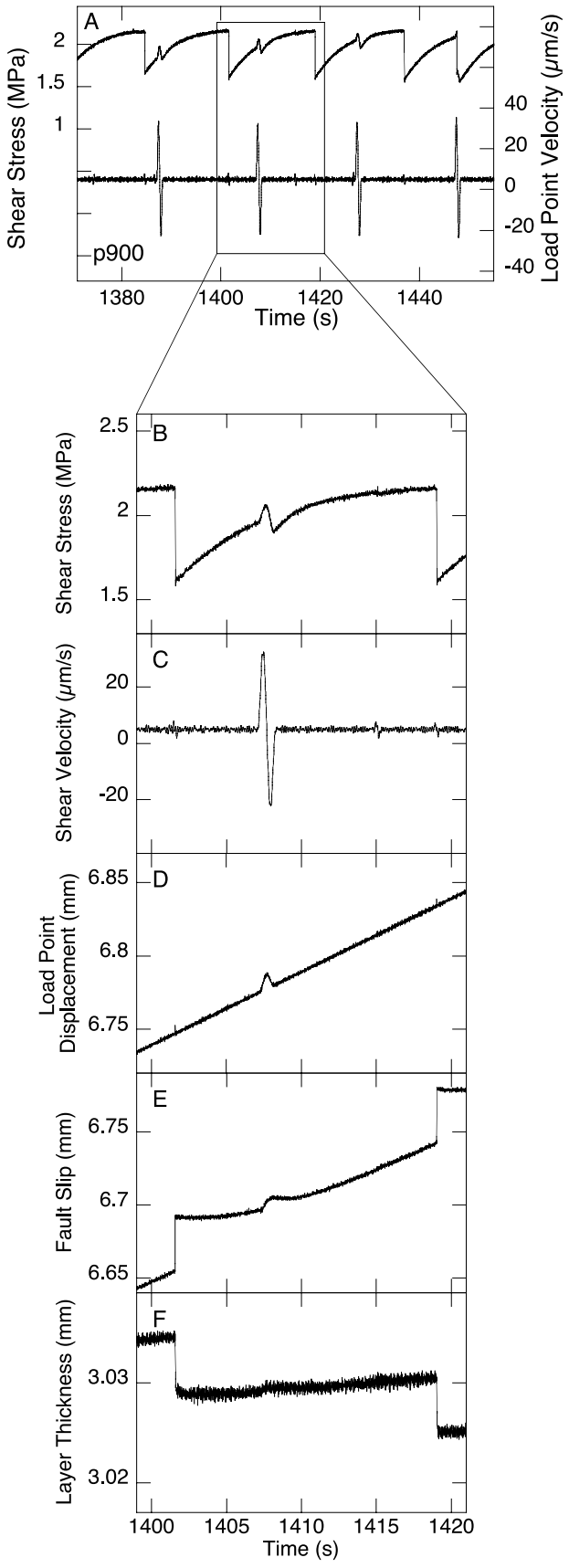

Figure 2. (a) Time series of shear stress and shear velocity. Note the shear stress response to the velocity oscillation. Transients that occur early in the seismic cycle do not trigger failure. A triggered event takes place at approximately 1445 s. (b) Time series of shear stress. (c) Time series of shear loading velocity. Transient stressing was implemented using a sinusoidal oscillation superimposed on a constant shear velocity of 5 μm/s. (d) Time series of load point displacement. (e) Time series of fault slip. (f) Time series of layer thickness. Positive change in layer thickness indicates dilation.

smoothed by wear during subsequent experiments (smooth granite experiments, Table 1).

3. Results

[9] We compare the recurrence interval, t_r, defined as the time between the onset of dynamic failures (Figure 3), of stick-slip under transient loading to recurrence intervals under constant loading conditions. Because the transient generally reduces the time to failure, the recurrence interval of triggered events should be measurably smaller than under constant loading. We refer to this as a positive clock advance. To understand the importance of both fault zone properties and properties of transient stressing, we vary the transient signal in our forcing function for all fault zone configurations. We also change where in the seismic cycle the transient oscillation occurs. It is convenient to define the parameter time-of-transient deformation (t_{trans}) as the origin time of the transient relative to the onset of the previous dynamic failure (Figure 3). In this way, we quantify the transient's position in the interseismic cycle. We measure stress drop of each event as the difference between the shear stress at the onset and the end of dynamic failure.

[10] Under constant loading conditions, stick-slip recurrence intervals are remarkably consistent for both glass beads [*Savage and Marone*, 2007] and granite surfaces. Recurrence rates depend not only on load point velocity, but also on the properties of the fault zone (Figure 4). Shear surfaces with and without gouge display a linear increase in stress immediately after a stick slip, which reflects the combined elastic stiffness of the machine and sample. As loading progresses there is a distinct break in the loading curves, which reflects the onset of inelastic stressing and creep. The inelastic yield point decreases systematically with increasing roughness and gouge layer thickness (Figure 4). Smooth granite surfaces show a kink in the loading curve close to failure (Figure 4a) whereas rough granite surfaces show a kink about halfway through the stick-slip cycle (Figure 4b). We interpret this as the onset of fault slip at asperity contacts [e.g., *Biegel et al.*, 1992]. Granular layers show a more prolonged transition to dynamic failure, which reflects the time (and slip) necessary for interparticle slip and rolling to extend across the layer. The transition period and the degree of inelastic creep increases with layer thickness (Figures 4c and 4d), which results in an increase in stick-slip recurrence interval. The stick-slip failure strength and the dynamic, minimum strength also decrease with increasing layer thickness (Figures 4c and 4d). Layer thickness does not affect stress

Table 1. List of Experiments

Experiment	Layer Thickness (mm)	Amplitudes (μm/s)	Frequency (Hz)	Duration (s)	Normal Stress (MPa)
p852	3	15,30,40,60	1	1	5
p900	3	30,40,60,80,120	1,2,3	1	5
p908	3	30,40,60,80	1,2,3	1	5
p923	3	40,80,120	1,2,3	0.33,0.5,1	5
p936	rough	15,25,35,50,75	1,2,3	1	5
p937	3	40,80,120	1,2,3	0.33,0.5,1	5
p961	6	15,25,40,60,80,120	1,2,3	1	5
p997	3	3,5,10,15	1	1	5
p1000	6	5,15,25,160	1,4	1	5
p1001	2	5,10,15,20,30	1	1	5
p1145	3	20,60	1	1	10
p1146	rough	60	1	1	10
p1165	3	40,80,120,160	1,2,3,4	1	5
p1166	smooth	35,40,80,120,160	1,2,3,4	0.25,0.33,0.5,1	5
p1172	smooth	40,80,120,160	1,2,3,4	0.25,0.33,0.5,1	5
p1173	smooth	40,80,120,160	1,2,3,4	0.25,0.33,0.5,1	5
p1176	2	5,10,15,20,30,40,60	1	1	5
p1177	6	15,20,30,40,50,60	1	1	5
p1178	smooth	5,10,30,40,50	1	1	5
p1227	smooth	5,40,80,120,160	1,2,3,4	1	5

drop (except for the smooth granite surface) and healing effects are minimal over the small changes in recurrence interval under constant loading (Figure 4e).

3.1. Definition of Triggering

[11] We employ a two-part definition of triggering for our experiments. First, the instability must occur during the transient deformation. Events that satisfy this criterion are shown by the closed symbols in Figure 5, where recurrence interval is plotted against timing of the transient deformation. By our definition of triggering, the events define a straight line and demonstrate the consistency of the time between trigger and stick slip. This time is dictated by the frequency of the stress oscillation, and because our minimum frequency is 1Hz, all transients reach peak stress in less than one second. The second part of our triggering definition requires that the recurrence interval of the earliest triggered event (Figure 5) for a given set of conditions must be two standard deviations away from the average recurrence interval for the same conditions under constant loading. This is to ensure that the events we call "triggered" actually represent a measurable clock advance. The average value and standard deviation are calculated from about 30 stick slips for each set of parameters. The earliest triggered event represents the shortest recurrence interval possible for a set of boundary conditions. This instability is important because it represents the greatest clock advance that can occur. This second part of the triggering definition becomes important when deciphering the amplitude threshold of triggering, as is seen in Figure 6.

3.2. Influence of Fault State

[12] Triggering sensitivity depends on when the transient occurs during the interseismic cycle (Figures 3 and 5). The data points at the top left of Figures 5a–5c (open symbols) represent cases where the transient occurs early in the stick-slip cycle and does not trigger failure. In these cases the recurrence time falls within the normal recurrence interval range. Once the fault has reached a critical state, almost all events occur during the transient. This is shown by the abrupt shift between nontriggered and triggered events (e.g., at a time since failure of 3.5 s in Figure 5a). Interestingly, there is no precursory change in the recurrence rate from the average, even immediately before the fault reaches its critical state. For example, if the transient had a weakening effect on the fault surface, which was small enough so that slip was not triggered immediately, we might expect to see decreasing recurrence rates before triggering during the transient began. This implies that our experiments do not show delayed triggering effects, as seen in nature when a fault fails after the seismic wave has passed. The clustering of triggered events around the average recurrence time is an artifact due to how the transient was imposed on the sample.

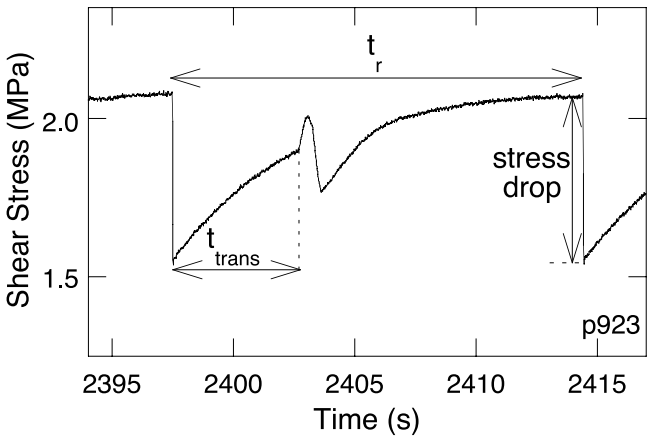

Figure 3. Time series for a stick-slip event and definitions of the measured parameters. Recurrence interval is the time between the onset of dynamic failures. Shorter recurrence intervals (relative to the average for constant loading) represent clock advance. Time of transient represents how far into the interseismic period the transient deformation occurs. Stress drop measures the shear stress released during dynamic failure.

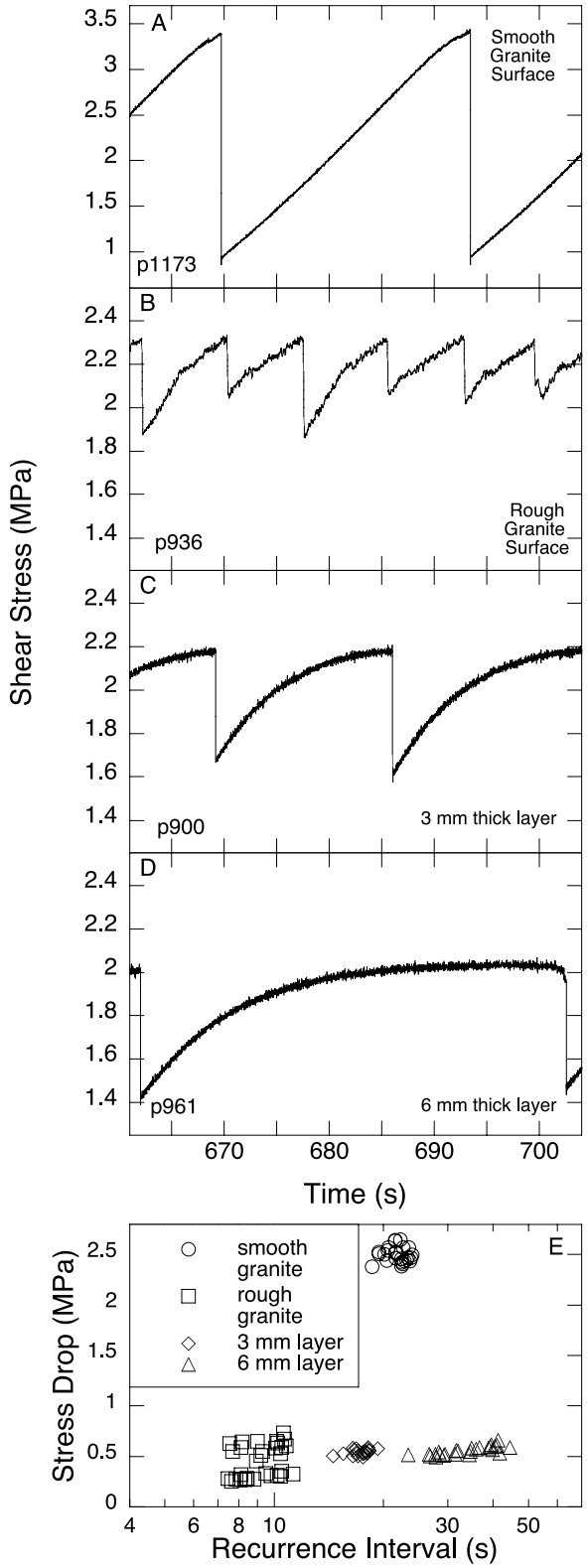

Figure 4. Stick-slip cycles for different fault zone architectures: (a) smooth granite surfaces, (b) rough granite surface, (c) 3-mm glass bead layer, and (d) 6-mm glass bead layer; (e) stress drop over recurrence interval for the experiments shown in Figures 4a–4d under constant loading condition.

When the time between transients and the average recurrence interval are similar, failure can become phase locked with the signal.

3.3. Transient Amplitude Effects and a Triggering Threshold

[13] As can be seen from the timing of the earliest triggered event in Figure 5, larger amplitudes produce greater clock advance. We plot the recurrence interval of the earliest triggered events versus amplitude to quantify this effect among different fault types (Figure 6). The zero amplitude point is the average recurrence interval without transient oscillations. The error bars represent two standard deviations. Triggered events are shown as solid symbols and open symbols are nontriggered events; the boundary between the open and closed symbols represents the triggering

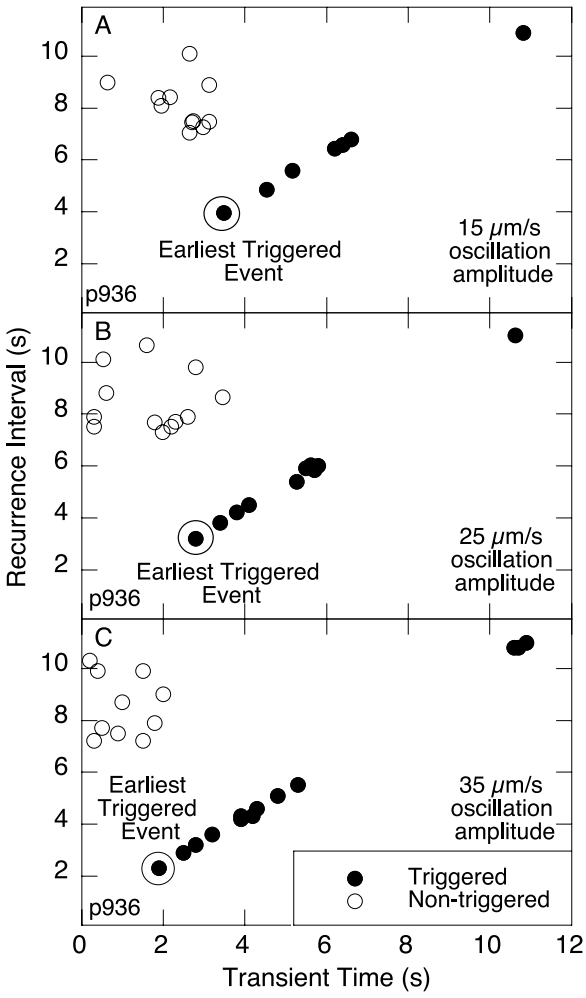

Figure 5. Recurrence interval is plotted versus transient time. Stress transients that occur near the beginning of the interseismic period do not trigger failure. We chose the earliest triggered events (shortest recurrence interval) to demonstrate the effects of oscillation amplitude and frequency on triggering. The small clustering of late triggered events represents the time between transients and therefore is merely an effect of experimental design. If time between transients was randomized, this effect would disappear.

threshold. Below certain amplitudes of the transient stress, the recurrence interval of triggered events is not statistically different from background values. This is the second part of our triggering definition above. We plot the amplitude thresholds outlined in these experiments as a function of gouge layer thickness (Figure 6e). The bars represent the range of possible thresholds (which is the range between the correlated and uncorrelated points in Figures 6a–6d. The triggering amplitude threshold decreases with increasing gouge layer thickness. The granite surfaces show a low threshold, although the threshold for rough surfaces is not well constrained (Figure 6a). Note also that the thickest gouge layers (Figure 6d) exhibit a greater rate of clock advance with increasing amplitude than thinner layers. Indeed, smooth granite surfaces show little change in recurrence interval with increasing amplitude.

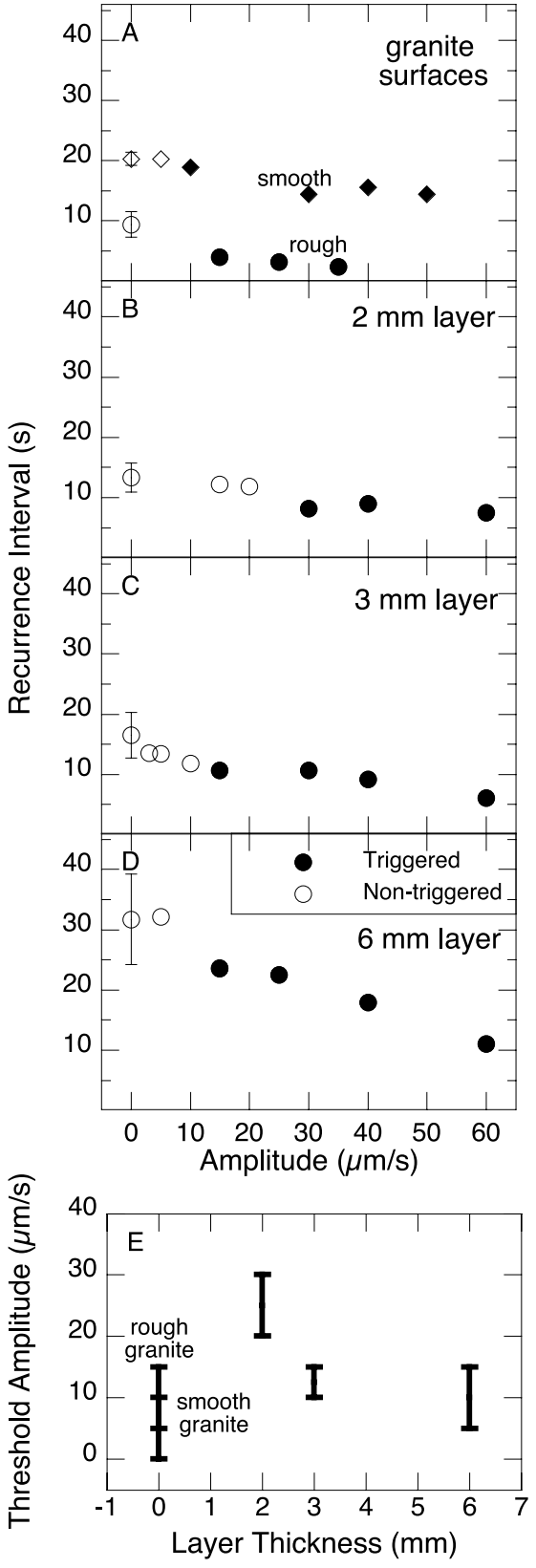

Figure 6. Recurrence interval for the earliest triggered events (Figure 5) versus transient stressing amplitude. Frequency is held constant at 1 Hz. Each point represents a result from a data set such as in Figure 5. The recurrence interval at zero amplitude represents the average for constant loading rate and error bars show ±2 standard deviations. The closed symbols represent recurrence intervals that are two standard deviations from the mean value at zero amplitude, which meet our criteria for triggering. Figure 6e shows a summary of threshold amplitudes for Figures 6a–6d.

[14] When considering fault state and triggering thresholds, it is useful to think not only in terms of absolute change in recurrence times, but also in terms of the recurrence of the earliest triggered event normalized by the average recurrence interval under constant loading rate (Figure 7). In this way, we can compare where in the interseismic cycle triggering commences for fault types with different recurrence intervals. For constant loading rate, the average recurrence time of a fault is determined by fault zone thickness, with thicker fault zones showing longer recurrence times. Figure 7 shows the data from Figure 6; however, recurrence interval is normalized by the average recurrence time for that experiment. In this plot, the zero amplitude point would plot at 1 on the normalized time since failure axis, representing a full interseismic cycle. Error bars represent uncertainty in the average recurrence. Figure 7 shows that larger amplitudes trigger events earlier in the seismic cycle, but that this effect is enhanced for thicker granular layers. The 2-mm-thick granular layers show that for the largest amplitude tested (60 μm/s), triggered events commence roughly halfway through the seismic cycle, whereas triggering commences at ~30% of the background recurrence interval for 3 and 6 mm layers. For the smooth granite surfaces, triggered events begin at ~80% of the background interseismic interval and show almost no variation with the amplitude of the transient stressing.

3.4. Transient Frequency and Duration Effects

[15] In order to isolate the effects of frequency from those of amplitude, we varied the dynamic forcing frequency for a constant transient stress amplitude. To do this, we increased the transient shear velocity for higher frequencies so as to keep a constant shear stress amplitude of approximately 0.12 MPa (Figure 8a), except for the roughened granite surface experiment where stress amplitude is smaller. Figure 8 shows the earliest triggered event for each

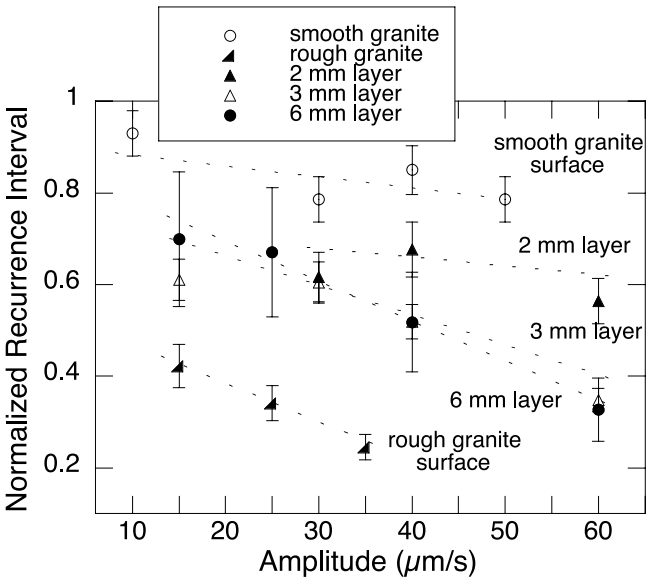

Figure 7. Recurrence intervals of earliest triggered events normalized by background recurrence interval versus transient stressing amplitude. Dashed lines approximate the slope for each fault configuration and suggest that the change in recurrence interval for thinner layers is less affected by transient amplitude.

frequency; all events fit our two-part definition of triggering. The uncertainty in the recurrence time for an individual event is small (hundredths of a second), therefore slight changes in recurrence time are meaningful. Six-millimeter-thick layers show increasing clock advance as frequency is increased, indicating that the layers are more susceptible to triggering from high frequencies (Figure 8b). Three-millimeter-thick layers also show increasing positive clock advance with increasing frequency (Figure 8b). Data for granite surfaces show a pronounced effect of roughness (Figure 8c). The frequency of transient stressing has different effects on smooth granite surfaces than on faults with gouge layers. Smooth granite surfaces show an initial decrease in recurrence interval and then a slight increase with increasing frequency. For rougher granite surfaces, recurrence intervals indicate a slight increase in clock advance with increasing frequency, although the noise in this experiment was significant. All experiments with transient stressing showed positive clock advance (Figure 8c).

[16] We again normalize the recurrence interval of the earliest triggered event by an average recurrence interval to compare the effects of the interseismic period on transient triggering between experiments with different average recurrence times (Figure 9). The effect of frequency is similar to that of amplitude, inasmuch as there is a greater clock advance in thick gouge layers compared to thinner layers. Smooth granite surfaces show at most a 20% change in recurrence interval, whereas rougher surfaces show up to a 90% change as a function of transient loading. The rougher surfaces experiments were conducted at a lower transient stress amplitude than the other experiments and we should note that if these experiments were run at a comparable stress amplitude, the clock advance would be even greater. The three mm layer experiment shows slightly less dependence of triggering on frequency than the six mm layer, but the two experiments are within error.

[17] To ensure that any frequency effects are not due to the number of stress oscillations, we varied the duration of dynamic stressing (Figure 10). For example, a transient of 1 Hz frequency and 1 s duration will produce one maximum stress peak, whereas a transient with a 3 Hz frequency and the same duration will produce three stresses above background (Figure 8a). We ran a series of experiments with varying frequency and duration of the transient, such that higher frequencies had shorter duration and each set of conditions produced one oscillation peak (Figure 10a). Transient stressing caused positive clock advance and shorter recurrence interval as a function of higher frequency,

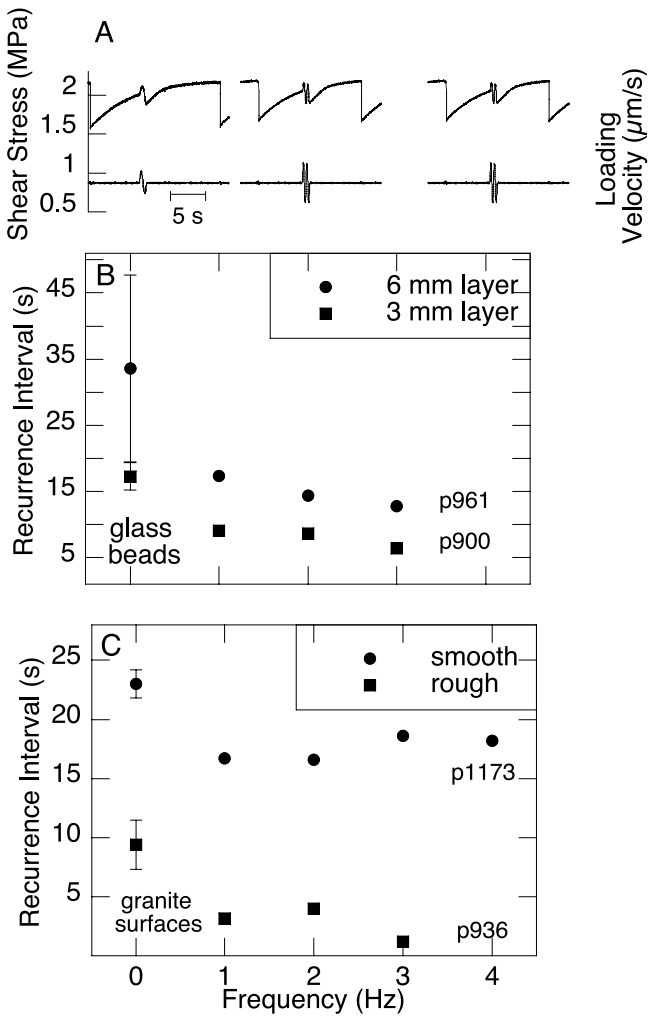

Figure 8. (a) Time series of 1-, 2-, and 3-Hz velocity oscillations and their effect on shear stress. Shear velocities are 40, 80, and 120 μm/s for 1-, 2-, and 3-Hz signals, respectively, in order to keep a constant shear stress amplitude. (b) Recurrence interval plotted versus frequency shows that granular layers are more susceptible to triggering from transients with high-frequency waves, (c) whereas granite surfaces show no effect or a dampening in susceptibility with increasing frequency. Error bars represent two standard deviations from the average recurrence at background loading rates.

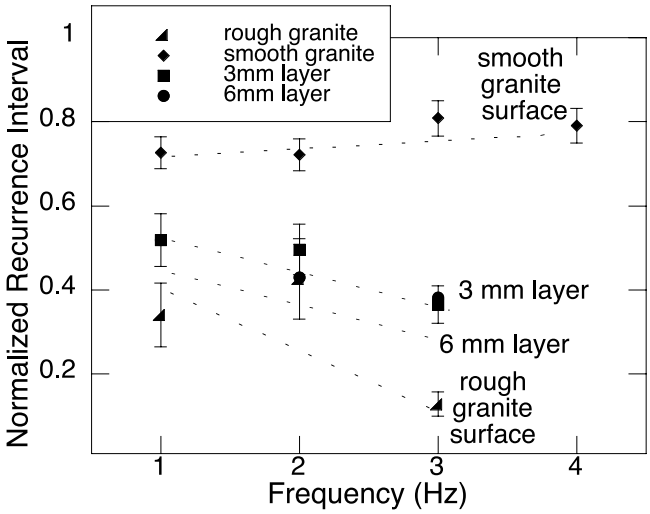

Figure 9. Recurrence interval of the earliest triggered event normalized by background recurrence interval plotted versus transient stressing frequency. Dashed lines approximate the slope for each fault configuration and suggest that thinner layers are less affected by transient frequency.

but the variable duration experiments are not statistically different from those with constant 1-s duration. (Figure 10b). This result is perhaps not surprising because all triggered events fail during the first peak in stress, regardless of transient frequency. However, similar studies conducted under continuous oscillations show triggering at lower amplitudes, indicating that much longer vibration durations have a significant weakening effect [*Savage and Marone*, 2007].

3.5. Effects of Transient Deformation on Stress Drop

[18] In addition to influencing the timing of instabilities, transient deformation also affects the magnitude of the stick-slip stress drop, compared to the size of nontriggered events (Figures 11a–11d). Previous work shows that stress drop increases with the log of stick-slip recurrence time [e.g., *Dieterich*, 1972; *Karner and Marone*, 2001] which is due to increased healing between surfaces in contact for longer periods. Our data indicate that triggered events (such as the closed symbols in Figure 5) have larger stress drops for a given recurrence interval than nontriggered events (Figures 11a–11d). In all fault zone types, the triggered events plot to the left and above the nontriggered events, meaning that triggered events show larger stress drops. Triggered events on the granite surface and 2-mm granular layer show an increase in stress drop with increasing recurrence interval; however, the two thicker gouge layers indicate a more constant stress drop at all recurrence intervals. We also plot the shear stress at failure for the 2-mm layer experiment (Figure 11e) that shows that the increase in stress drop seen for the triggered events is due in part to increased failure strength, demonstrating a failure threshold that is a function of loading velocity, rather than a constant Coulomb-style failure threshold or a Coulomb threshold modified by healing effects with contact time. Healing effects do account for the increase in strength with recurrence interval seen within the triggered and nontriggered groups but not for the failure strength differences between groups.

[19] We also investigate whether the amplitude and frequency of the transient affect the size of the stress drop. These data bear on the question of whether the magnitude of the triggering earthquake influences the size of the triggered event. Figures 12 and 13 show the average stress drop as a function of amplitude and frequency for several experiments. For the granular faults, amplitude has no effect on stress drop (Figures 12b, 12c, and 12d), whereas higher frequency transients may cause slightly greater stress drops (Figures 13b and 13c). However, the bare granite surfaces show a slight increase in stress drop with increasing amplitude (Figure 12a), but no trend with frequency (Figure 13a). The slight trends in Figures 12a, 13b, and 13c are very subtle and when considering the standard deviation of our results, arguably nonexistent, indicating that the size of the triggering earthquake does not determine the size of the triggered earthquake.

4. Discussion

[20] Our results imply that earthquake triggering depends both on the amplitude and frequency of the transient deformation, as well as properties of the fault zone. Larger amplitude stresses correlate with decreasing recurrence interval on granular layers. Faults with granular layers also tend to have shorter recurrence rates at higher frequency whereas the recurrence intervals of granite surfaces are lengthened or unaffected by high-frequency oscillations. Because loading conditions were similar for all experiments, we can assume that the systematic variations we see with respect to amplitude and frequency are related to physical properties of each fault zone type. Studies of failure on frictional surfaces indicate that a small amount

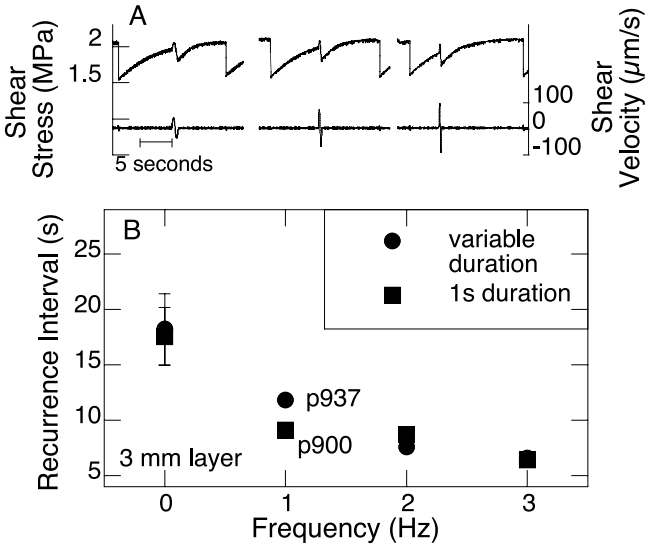

Figure 10. Effects of transient duration on recurrence interval. (a) Time series showing 1, 2, and 3 Hz transient oscillations of 1, 0.5, and 0.33 s duration and their effect on shear stress. (b) Effect of transient duration and frequency on clock advance. Note that the effects of frequency are independent of oscillation number.

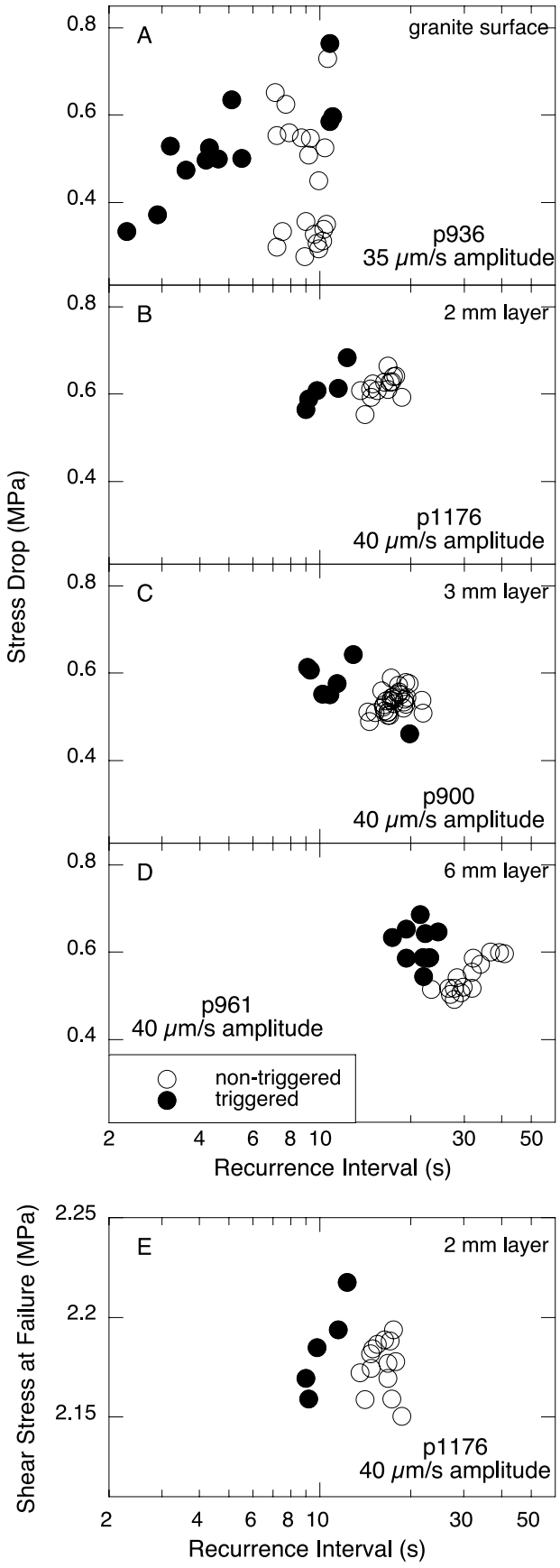

Figure 11. (a–d) Stress drop over recurrence interval for both triggered and nontriggered stick slips. Triggered events have larger stress drops per recurrence time than nontriggered events. (e) Shear stress at failure over recurrence interval (showing the same experiment as Figure 11b). The increase in stress drop with respect to recurrence interval shown for the triggered events is due in part to higher failure stresses for triggered events.

of inelastic slip, known as the critical slip distance (D_c), must occur before a surface fails unstably. According to rate and state friction theory, the critical slip distance is proportional to the displacement needed to renew asperity contact junctions [*Rabinowicz*, 1951; *Dieterich*, 1979]. For bare granite surfaces, D_c is proportional to mean asperity size. For granular layers, the critical distance is proportional to shear band width and mean grain size, because all of the grain contacts within a shear zone or granular force chain must be renewed [*Marone and Kilgore*, 1993; *Marone*, 1998; *Savage and Marone*, 2007]. To determine why amplitude and frequency of transient stressing have different effects on granite surfaces and granular layers, we investigate the relationship between critical friction distances for the various experimental fault zones.

4.1. Critical Displacement Lengths and Transient Effects

[21] Because a fault must weaken prior to failure in the context of slip or velocity weakening, a fault slip distance proportional to D_c must be achieved during triggering by transient stressing. The critical slip distance may be the parameter that modulates the sensitivity to triggering. If the amplitude threshold is related to D_c, then we can assume that for a transient deformation to trigger an event, the transient-induced slip must be greater than or equal to D_c. We posit that the variations in amplitude threshold observed in our experiments (Figure 6) represent this effect. Because of inelastic creep prior to failure, the threshold most likely represents the summation of the displacement during the transient and any recent or ongoing creep displacement, which may be why timing of the transient in the interseismic period has a larger role in determining clock advance in granular layers (Figure 7). For gouge layers, creep displacements increase during most of the interseismic period (unlike the granite layers which creep much less during the interseismic period). Therefore the transiently induced slip needed to achieve D_c becomes smaller as the interseismic period progresses, which explains why smaller transients can trigger events later in the interseismic cycle (such as in Figure 6d). In comparison, triggering of the granite surfaces and thin gouge layers is not as strongly influenced by fault state relative to the interseismic period. This indicates that the "critical state" at which faults are susceptible to triggering can be achieved late in the interseismic cycle (as in the smooth granite surfaces) or it can be a function of the transient amplitude and achieved after only a fraction of the interseismic period has passed.

[22] Our data show that triggering by transient stresses also varies with frequency and fault zone thickness (Figure 8). High frequencies had the largest effect on thicker gouge layers. The granite surface experiments hint that

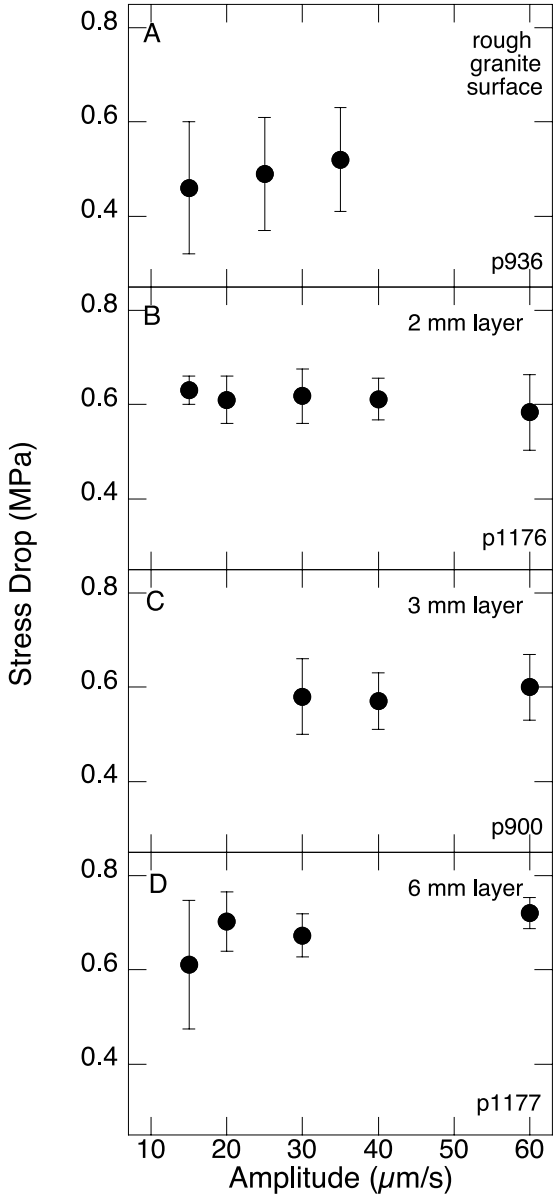

Figure 12. Average stress drop over amplitude for (a) granite surfaces, (b) 2-mm layer, (c) 3-mm layer, and (d) 6-mm layer. Error bars are ±2 standard deviations from the average. Only the granite surfaces show any correlation between the size of the event and the amplitude of the triggering event. Transient frequency is 1 Hz in all cases.

increasing frequency may reduce clock advance. We hypothesize that the effects of frequency result from systematic variation of D_c with fault zone thicknesses and that the difference in frequency effects as a function of fault type (Figure 8) results from differences in load point velocity when the critical displacement has been reached. Because our transient load point velocity is a sinusoid, velocity can be either increasing or decreasing as the fault fails. According to rate and state friction theory, when velocity increases, frictional strength increases as well and then decays to a new value as slip accumulates. Similarly, a decrease in velocity instantaneously lowers the frictional strength of the fault. This increase or decrease in fault strength, just as the fault is ready to fail (i.e., the fault has slipped D_c), could hinder or enhance triggering.

[23] To demonstrate that there is indeed a change in load point velocity phase at failure, we plot the phase as a function of frequency (Figure 14). Data points represent the velocity phase at failure for the events shown in Figure 8. The velocity peak is defined as zero phase, such that negative phase indicates failure during increasing velocity and positive phase indicates failure during decreasing velocity. The smooth granite surfaces fail before the velocity peak except at 2 Hz frequency (although phase is very weakly positive). The three and six mm layers both fail after the velocity peak in all cases, and have similar phase to each other.

[24] Because of this correlation between fault type and timing of failure with the load point velocity, we compare the effective critical displacement of each fault type with the load point displacement at peak velocity to determine if the direct effect of rate and state friction affects triggering. We measure the fault slip that occurs after the onset of the transient and before dynamic failure begins (Figure 15a), and use this displacement as a proxy for D_c. This displace-

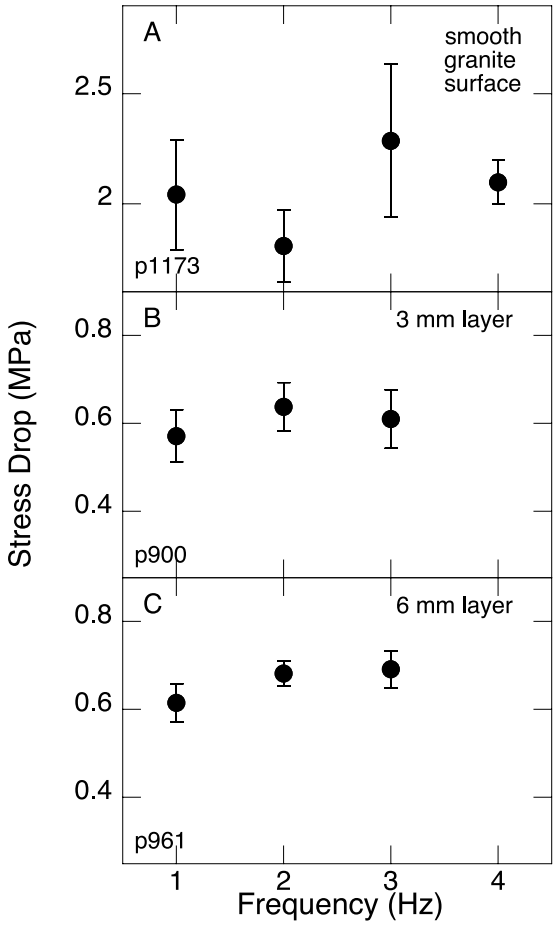

Figure 13. Average stress drop over frequency for (a) granite surfaces, (b) 3-mm layer, and (c) 6-mm layer. Error bars are ±2 standard deviations from the average. Stress amplitude is approximately 0.12 MPa for all experiments; load point velocity amplitude increases with increasing frequency.

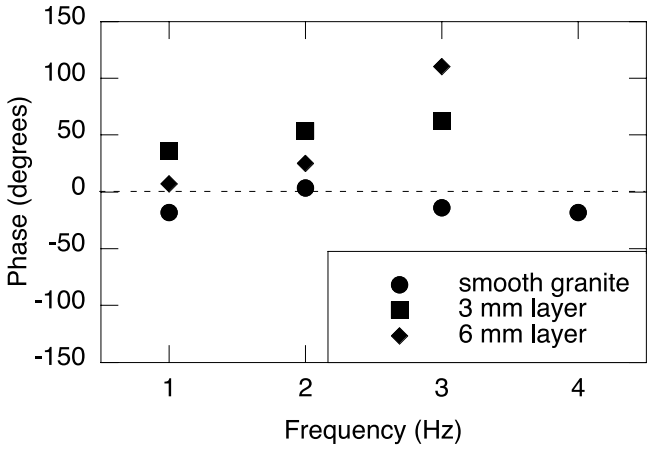

Figure 14. Load point velocity phase of stick-slip failure. Smooth granite surfaces fail before load point velocity peaks, whereas granular layers fail post peak.

ment, which we call effective D_c, is most likely larger than D_c; however, effective D_c should be a function of the true value. Fault slip is calculated by correcting the load point displacement for elastic effects of the loading apparatus. As shown in Figure 4, inelastic slip begins prior to failure in all cases, and therefore our estimates of effective D_c represent lower bounds on the true values. To minimize this effect, we only use slip values for the earliest triggered events for each fault type. This ensures that most of the preinstability slip occurs during the transient and not beforehand. Where possible, we measured slip for the earliest triggered events at different transient velocity amplitudes (but equal stress amplitudes) so that our D_c values represent an average for each fault type. For two cases, we use the largest amplitude tested for that fault type and not an average (shown as points without error bars in Figure 15b).

[25] Figure 15b shows D_c for each fault type as a function of the load point displacement at peak loading velocity during the transient. The reference line shows where the load point displacement at peak velocity equals D_c. The critical displacements for granite surface experiments p1173 and p1166 were in fact too small to measure accurately, so we assume they are smaller than 1 μm as this is near our slip resolution above the noise level in these data. In these experiments, D_c is less than the load point displacement when transient velocity peaks (left of the line in Figure 15b) and therefore the fault slip velocity is increasing as the surface begins to fail. This increasing velocity should result in transient strengthening via the friction direct effect. Because we use larger velocity amplitudes at higher frequencies to maintain constant stress amplitudes, the change in velocity is greater at higher frequencies. The thickest gouge layer experiments fall well to the right of the line, meaning that velocity is decreasing as the layer fails and likewise the transient strength of the material decreases, due to the friction direct effect. This negative velocity excursion results in reduced frictional strength. As shown in Figure 8, thicker gouge layers show the greatest clock advance. The thinner gouge layer and roughened granite surface experiments fall close to the reference line so that velocity is near or just past its peak. Because velocity is not changing at the peak, there is not a significant change to the strength of the layer. These experiments showed the smallest change in clock advance due to frequency effects.

[26] Previous studies have indicated that earthquake triggering is frequency independent when the oscillation frequency is above the critical frequency [*Lockner and Beeler*, 1999; *Beeler and Lockner*, 2003; *Savage and Marone*, 2007]. The critical frequency is the inverse of the time needed to slip the critical friction distance. In theory, above this frequency, the stress amplitudes need to be much larger than predicted by simple failure models in order to trigger earthquakes. This change in triggering thresholds between high and low frequencies has been used to explain why tidal oscillations and some large earthquakes do not trigger seismicity [e.g., *Scholz*, 2003]. According to standard thinking, if the period of the oscillation is shorter than the nucleation time, the effect of the oscillation on friction is no longer phase coherent, and therefore friction could be increasing or decreasing [e.g., *Dieterich*, 1994; *Scholz*, 2003; *Beeler and Lockner*, 2003]. This would be true for all frequencies above the critical frequency, so that failure is independent of frequency. Our frequency range is above the critical frequency in most experiments (except smooth

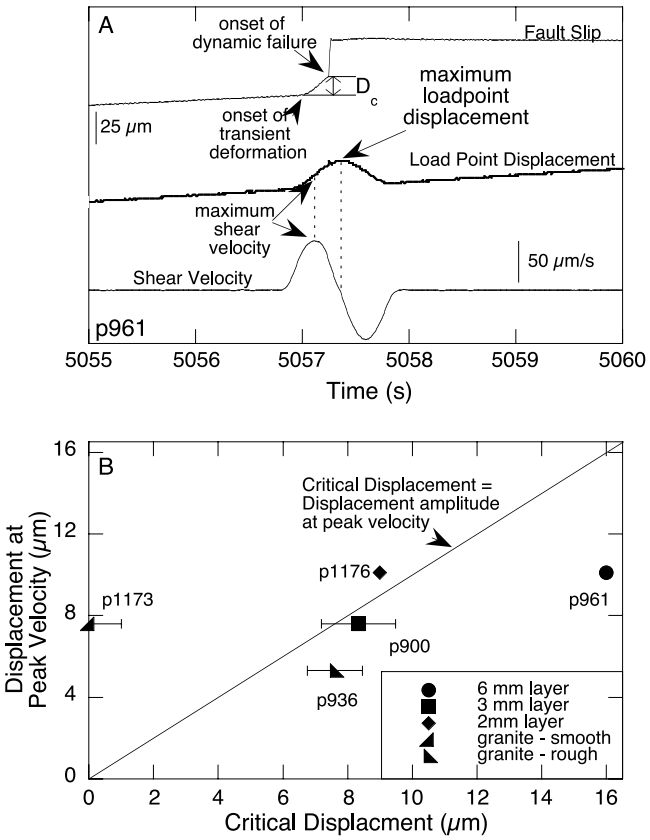

Figure 15. (a) The fault slip that occurs after the onset of the transient deformation but before the onset of dynamic failure is an approximation of the critical displacement. We also demonstrate that the maximum shear velocity occurs at $\pi/2$ in the transient displacement oscillation. (b) The average value of D_c measured for all triggered events in different fault configurations. The error bars represent one standard deviation.

Table 2. Model Parameters

a	b	Dc (μm)	V_{lp} (μm/s)	T_r (s)	Time Since Failure (s)	Amplitude (μm/s)	Frequency (Hz)	k = k_c (1/μm)
0.01	0.014	1	5	2.12	~2	10, 20, 40, 50, 80, 100	1–10	0.004

granite surfaces); however, our results show that frequency in most cases affects phase at failure. We propose that the immediate change in strength due to a transient change in slip velocity affects the triggering potential at certain frequencies, but that it can reduce or strengthen the potential depending on the value of D_c.

[27] The smooth granite surface experiments in Figure 8b suggest that at higher frequencies than we tested, not only would triggering cease but failure may be inhibited as well by high-frequency vibrations. The experiments of *Beeler and Lockner* [2003] were also conducted on granite surfaces and show a frequency strengthening effect. We suggest that for the behavior of a fault to be independent of stressing frequency, the transient load point displacement amplitude at peak velocity must be equal to D_c. Our hypothesis suggests that any fault can exhibit strengthening, weakening or independence, but that the thresholds for each of these behaviors will depend on the length of D_c. For example, thick granular layers would show frequency strengthening at larger amplitudes than tested in this study.

[28] The strengthening of the layer with a positive velocity excursion can also explain why the triggered events have larger stress drops compared to their non-triggered counterparts. Even events that fail as velocity is decreasing still fail when the velocity is greater than the background rate (5 μm/s) so that some strengthening occurs in every triggered event. This indicates that triggered events are larger in magnitude than if the fault had failed with a constant tectonic loading rate. The lack of a convincing trend in the change in stress drop with amplitude or frequency, however, supports studies of seismic data showing that the size of the triggered event should be independent of the size of the triggering earthquake [*Felzer et al.*, 2004].

4.2. Rate and State Friction Models

[29] In order to understand how D_c affects the changes in clock advance at different amplitudes and frequencies, we evaluate our results in the context of rate and state friction laws [*Dieterich*, 1979; *Ruina*, 1983]. The constitutive law states that friction is a function of velocity and fault state, such that:

$$\mu = \mu_0 + a \ln\left(\frac{V}{V_0}\right) + b \ln\left(\frac{V_0 \theta}{D_c}\right) \tag{1}$$

$$\frac{d\theta}{dt} = 1 - \frac{V\theta}{D_c} \tag{2}$$

where μ_0 is the reference friction value, V_0 is a reference sliding velocity, V is the fault slip rate, D_c is the critical slip distance, θ is the state variable and a and b are empirically derived constants. Equation (2) is the Dieterich aging law for the evolution of the state variable [*Dieterich*, 1979], where the fault state can evolve while the fault is stationary. We describe the elastic interaction of our sample with our testing apparatus as:

$$\frac{d\mu}{dt} = k\left(V_{lp} - V\right) \tag{3}$$

where k is stiffness divided by normal stress and V_{lp} is the load point velocity. The parameters used for the model results are shown in Table 2. We attempt to capture our experimental conditions by using the same load point velocity and stiffness, as well as approximating a, b, and D_c from previous work on similar materials [*Mair and Marone*, 1999]. The frictional parameters are constrained so that the critical stiffness equals the system stiffness to create an unstably sliding system, similar to our experimental stick-slip conditions. The onset of unstable failure is defined as the maximum friction value before rapid slip. We use a range of transient amplitudes and a constant D_c to demonstrate the effects of load point displacement during the transient as a function of D_c (Figure 16a). Similar results could be obtained by holding the transient amplitude constant and varying D_c.

[30] The frequency effects on recurrence interval are shown in Figure 16b. In each of these models, the oscillation begins at the same time within the interseismic cycle. Below the smallest amplitude shown here, failure always occurs after the first oscillation peak. The models shown here fail during the first peak, similar to what we see in experiments, until the recurrence interval begins increasing again, which occurs at different frequencies for different amplitudes. The decrease in recurrence interval in the model occurs because higher frequencies reach their first maximum peak faster. The 0.18 MPa amplitude in Figure 16b shows that the recurrence interval decreases with increasing frequency until ten Hz, at which time the recurrence interval starts to lengthen again. The 0.11 MPa amplitude shows that same trend except that the recurrence interval decreases until two Hz. The increase in recurrence seen in the model results is always due to the fault failing after the first maximum amplitude peak, whereas our experiments always fail during the first maximum amplitude peak. Therefore, the model never demonstrates an increase in recurrence interval with frequency such as seen in the smooth granite block experiments. Indeed, the model always predicts a decrease in recurrence for events triggered at higher frequencies.

[31] The majority of the models fail as velocity is decreasing (positive phase lag). The exceptions are the two points showing the largest amplitude studied (we only show one and two hertz frequencies because the model was unstable at higher frequencies and we could not determine a recurrence interval). On the basis of our experimental results, we hypothesize that the increase or decrease in velocity during the transient deformation will temporarily increase or decrease frictional strength of the fault. To investigate this specifically, we look at the friction at the

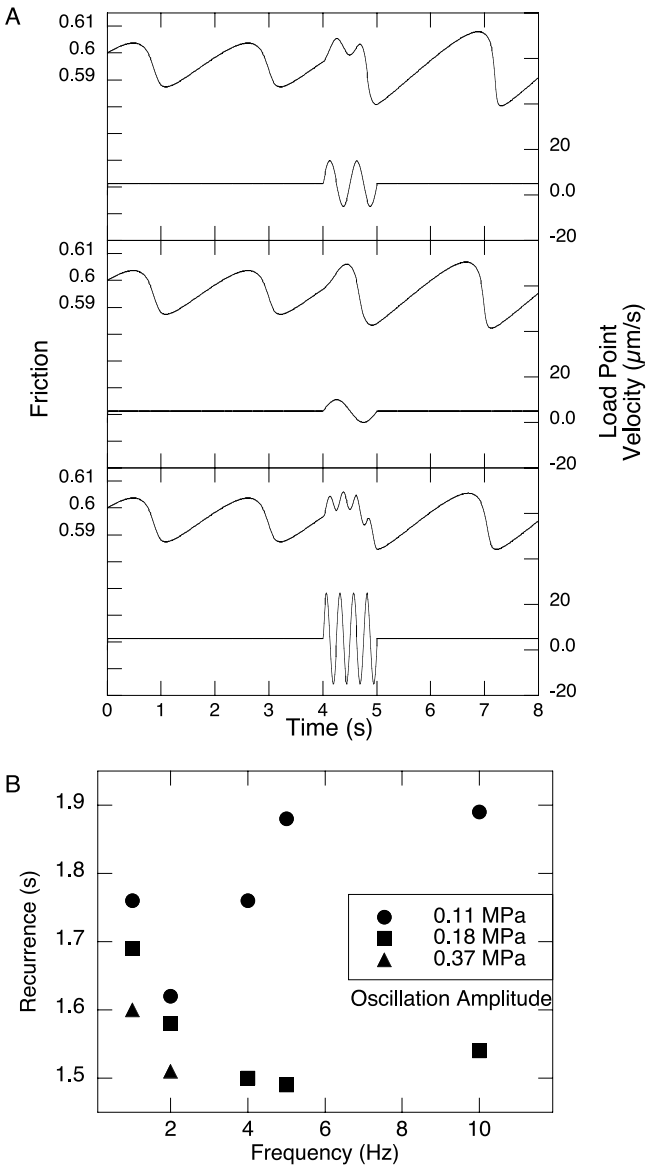

Figure 16. (a) Time series of frictional instabilities in our model. The velocity oscillation begins at 4 s in each frame. (b) Rate and state friction models of recurrence as a function of frequency.

onset of failure in our models (Figure 17). Friction values are positively correlated with frequency, regardless of whether the failure occurs as velocity is increasing or decreasing. From our hypothesis, we would expect to see events triggered at higher frequency to fail at lower friction values for the events with positive phase lag. Although the model does not show this, there is a decrease in strengthening at higher frequencies for decreasing oscillation amplitudes. For instance, there is almost no change in frictional strength at the lowest stress amplitude.

[32] The failure of the rate and state model to capture the increase in recurrence interval with frequency in the granite surface experiments could indicate that the changes in recurrence intervals are not due to the friction direct effect, although it is clear from the experimental results that recurrence interval is influenced by whether load point velocity is increasing or decreasing when failure occurs. A more extensive investigation of the rate and state friction theory, perhaps including a randomization of the model to more accurately capture the experimental conditions, could prove insightful.

4.3. Tectonic Implications

[33] Our experiments indicate that the apparent complexity of triggering (as indicated by differences in the effects of amplitude and frequency of transient stressing for different faults) may be the result of differences in fault zone properties. One of the most important implications is that the high-frequency threshold (failure threshold for oscillations higher than the critical frequency) may not be constant, as has been previously proposed. For faults with a thicker gouge zone, and hence larger D_c, the threshold may not be remarkably different from a threshold predicted by simple failure models, such as a Coulomb-type failure, and the triggering threshold at high frequencies could be quite low. Therefore, fault systems with a comparably low amplitude threshold may have faults with larger D_c.

[34] The difference in frequency response between the bare granite surfaces and the granular layers suggest an explanation for discrepancies in the observed effect of seismic frequency, as well as possibly providing a new way to estimate D_c for earthquake faults. For instance, the study at Long Valley Caldera [*Brodsky and Prejean*, 2005] found that earthquakes with enhanced low-frequency energy were more likely to trigger additional seismicity. The amplitude threshold listed by *Brodsky and Prejean* [2005] is between 0.04 and 0.08 cm/s for vertical amplitudes for wave periods longer than 30 s, giving a displacement threshold between 2 and 3.4 mm (when corrected to 3 km depth). Because they saw a transition from nontriggering to triggering at 30 s, we may assume that above this frequency, the critical displacement is not reached during the transient and earthquakes are not triggered. At periods longer than 30 s, the displacement during the transient becomes equal to or greater than D_c and events are triggered. The faults at Long Valley should have minimal gouge layers; we might assume that these faults are immature because the source of their

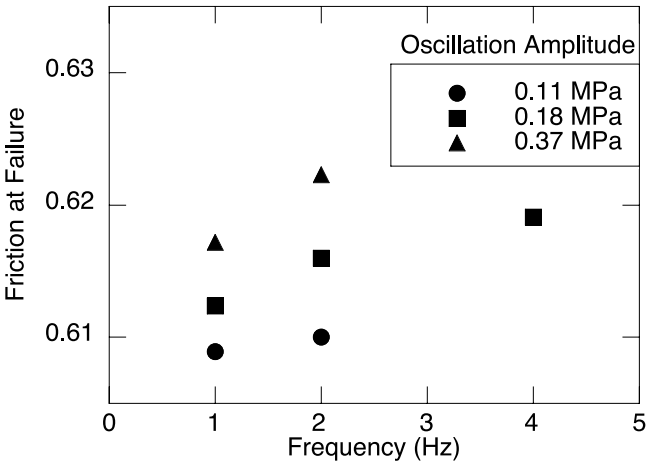

Figure 17. Friction as a function of frequency for rate and state friction model. Models where failure occurred after the first load point velocity peak are not included.

activity is the recent volcanism in the area. Their shallow seismicity may also be an indication that the faults have a limited gouge layer. *Marone and Scholz* [1988] attributed the upper stability transition of 5 km depth to be due to the velocity strengthening behavior of unconsolidated gouge layers; however, faults lacking a significant gouge layer can nucleate earthquakes at shallower depths. The critical displacement length in this area may be approximately 2–3.4 mm and is more likely controlled by surface roughness of the faults, which is a reasonable assumption for faults with small total shear strain.

[35] The ratio of background velocity to sinusoid velocity for the laboratory thresholds is about 1 for most of the fault types investigated, whereas the ratio of tectonic plate rate to seismic wave velocity thresholds (for the faults at Long Valley) is closer to 1×10^{-7}. This discrepancy indicates that laboratory faults are more sensitive to triggering, most likely due to the idealized fault geometry in the lab. Furthermore, our experiment is unlike natural faults in that the ratio of the duration of the laboratory transient to the recurrence interval is much larger than the duration of a seismic wave to the recurrence time on faults. However, because the amplitude of the seismic wave is so much larger, this difference is in effect diminished.

[36] Estimates of the critical displacement length for natural faults range over several orders of magnitude. Measurements of D_c in the lab are thought to scale up to earthquake faults (which are rougher and have much wider gouge zones); however, *Abercrombie and Rice* [2005] argued that D_c values on some areas of a fault may be on the same scale as laboratory measurements (0.01 to 0.1 mm) but rougher patches such as step overs may require 0.5 mm of slip to instigate failure. More importantly, they suggest that weakening continues throughout slip, so that the value of D_c may not have much meaning. *Marone and Kilgore* [1993] estimated D_c values of 1 mm for active strands of mature fault zone (in this case the San Andreas) due to the effect of microstructural fabrics on strain distribution. Similarly, *Scholz* [1988] proposed D_c to be on the order of 1–10 mm on surfaces with fractal roughness. Estimates of D_c for small faults in gold mines are 0.1 mm and suggest that D_c scales with the thickness of the gouge zone [*Richardson and Jordan*, 2002]. *Ide and Takeo* [1997] found an upper limit of D_c at 50 cm from waveform inversions of the 1995 Kobe earthquake. *Mair and Marone* [1999] found that in laboratory experiments, D_c increases with a log increase in velocity.

[37] In our experiments we have focused on the triggering effects of shear oscillations; however, seismic waves will more likely impinge a fault at an angle, meaning that the fault will experience both shear and normal loading oscillations. Previous studies have generally found that faults weaken during normal load perturbation and quickly regain strength when constant load resumes [*Boettcher and Marone*, 2004; *Hong and Marone*, 2005; *Richardson and Marone*, 1999]. Dynamic weakening is greatest under large amplitude, high-frequency vibrations for granular materials [*Boettcher and Marone*, 2004], indicating that the clock advances seen in our granular experiments could be even greater under both shear and normal vibrations. The decrease in clock advance seen in our high-frequency granite surface experiments could be somewhat negated by an induced decrease in fault strength; however, it is not immediately clear whether the same dynamic weakening effect would occur on bare surfaces.

[38] Our experiments also fail to capture delayed triggering effects where there is a clock advance in failure; however, failure does not occur until after the wave train has passed. This observation could be due to various conditions and processes on the fault that our models fail to capture, such as migration of fluids [*Husen et al.*, 2004a].

5. Conclusions

[39] The triggering potential of a transient deformation on shear surfaces depends on the amplitude and frequency of the wave, as well as the properties of the fault zone. Larger-amplitude events generally increase clock advance of earthquakes; however, greater changes in clock advance are witnessed on faults with greater interseismic creep. Bare surfaces are more susceptible to triggers where energy is concentrated at low frequencies, whereas gouge layers are encouraged to fail by high frequencies. The threshold between the different frequency responses seems to scale with maximum load point displacement during transient deformation and the critical slip length. Triggered events have larger stress drops than nontriggered events with the same recurrence time. The velocity amplitude of the transient has little discernible effect on stress drop, meaning that the size of the triggering earthquake may not have an effect on the size of the events it triggers.

[40] **Acknowledgments.** This manuscript was greatly improved by reviews from Joan Gomberg, Steve Karner, and an anonymous reviewer. This work was supported by National Science Foundation grants EAR-0196570, OCE-0196462, EAR-0337627, and EAR-0345813 and by USGS/NEHRP award 05HQGR0025.

References

Abercrombie, R. E., and J. R. Rice (2005), Can observations of earthquake scaling constrain slip weakening?, *Geophys. J. Int.*, *162*, 406–424, doi:10.1111/j.1365-246X.2005.02579.x.

Beeler, N. M., and D. A. Lockner (2003), Why earthquakes correlate weakly with the solid Earth tides: Effects of periodic stress on the rate and probability of earthquake occurrence, *J. Geophys. Res.*, *108*(B8), 2391, doi:10.1029/2001JB001518.

Biegel, R. L., W. Wang, C. H. Scholz, G. N. Boitnott, and N. Yoshioka (1992), Micromechanics of rock friction: 1. Effects of surface roughness on initial friction and slip hardening in Westerly Granite, *J. Geophys. Res.*, *97*(B6), 8951–8964, doi:10.1029/92JB00042.

Boettcher, M. S., and C. Marone (2004), Effects of normal stress variation on the strength and stability of creeping faults, *J. Geophys. Res.*, *109*, B03406, doi:10.1029/2003JB002824.

Brace, W. F., and J. D. Byerlee (1966), Stick-slip as a mechanism for earthquakes, *Science*, *153*, 990–992, doi:10.1126/science.153.3739.990.

Brodsky, E. E. (2006), Long-range triggered earthquakes that continue after the wave train passes, *Geophys. Res. Lett.*, *33*, L15313, doi:10.1029/2006GL026605.

Brodsky, E. E., and S. G. Prejean (2005), New constraints on mechanisms of remotely triggered seismicity at Long Valley Caldera, *J. Geophys. Res.*, *110*, B04302, doi:10.1029/2004JB003211.

Brodsky, E. E., V. Karakostas, and H. Kanamori (2000), A new observation of dynamically triggered regional seismicity; earthquakes in Greece following the August, 1999 Izmit, Turkey earthquake, *Geophys. Res. Lett.*, *27*, 2741–2744, doi:10.1029/2000GL011534.

Byerlee, J. D., and R. Summers (1976), A note on the effect of fault gouge thickness on fault stability, *Int. J. Rock Mech. Min. Sci. Geomech. Abstr.*, *13*, 35–36, doi:10.1016/0148-9062(76)90226-6.

Dieterich, J. (1972), Time-dependent friction in rocks, *J. Geophys. Res.*, *77*, 3690–3697, doi:10.1029/JB077i020p03690.

Dieterich, J. H. (1979), Modeling of rock friction: 1. Experimental results and constitutive equations, *J. Geophys. Res.*, *84*(B5), 2161–2168, doi:10.1029/JB084iB05p02161.

Dieterich, J. (1994), A constitutive law for rate of earthquake production and its application to earthquake clustering, *J. Geophys. Res.*, *99*(B2), 2601–2618.

Engelder, J. T., J. M. Logan, and J. Handin (1975), The sliding characteristics of sandstone on quartz fault-gouge, *Pure Appl. Geophys.*, *113*, 69–86, doi:10.1007/BF01592900.

Felzer, K., and E. E. Brodsky (2006), Decay of aftershock density with distance indicates triggering by dynamic stress, *Nature*, *441*, 735–738, doi:10.1038/nature04799.

Felzer, K., R. E. Abercrombie, and G. Ekstrom (2004), A common origin for aftershocks, foreshocks, and multiplets, *Bull. Seismol. Soc. Am.*, *94*, 88–98, doi:10.1785/0120030069.

Gomberg, J., and S. Davis (1996), Stress-strain changes and triggered seismicity at The Geysers, California, *J. Geophys. Res.*, *101*(B1), 733–749, doi:10.1029/95JB03250.

Gomberg, J., and P. A. Johnson (2005), Seismology—Dynamic triggering of earthquakes, *Nature*, *437*, 830, doi:10.1038/437830a.

Gomberg, J., M. Blanpied, and N. M. Beeler (1997), Transient triggering of near and distant earthquakes, *Bull. Seismol. Soc. Am.*, *87*, 294–309.

Gomberg, J., P. A. Reasenberg, P. Bodin, and R. Harris (2001), Earthquake triggering by seismic waves following the Landers and Hector Mine earthquakes, *Nature*, *411*, 462–466, doi:10.1038/35078053.

Gomberg, J., P. Bodin, and P. A. Reasenberg (2003), Observing earthquakes triggered in the near field by dynamic deformations, *Bull. Seismol. Soc. Am.*, *93*, 118–138, doi:10.1785/0120020075.

Gomberg, J., P. Bodin, K. Larson, and H. Dragert (2004), Earthquake nucleation by transient deformations caused by the M = 7.9 Denali, Alaska earthquake, *Nature*, *427*, 621–624, doi:10.1038/nature02335.

Harrington, R. M., and E. E. Brodsky (2006), The absence of remotely triggered seismicity in Japan, *Bull. Seismol. Soc. Am.*, *96*, 871–878, doi:10.1785/0120050076.

Hill, D. P., et al. (1993), Seismicity remotely triggered by the magnitude 7.3 Landers, California, earthquake, *Science*, *260*, 1617–1622, doi:10.1126/science.260.5114.1617.

Hong, T., and C. Marone (2005), Effects of normal stress perturbations on the frictional properties of simulated faults, *Geochem. Geophys. Geosyst.*, *6*, Q03012, doi:10.1029/2004GC000821.

Hough, S. E., L. Seeber, and J. G. Armbruster (2003), Intraplate triggered earthquakes; observations and interpretation, *Bull. Seismol. Soc. Am.*, *93*, 2212–2221, doi:10.1785/0120020055.

Husen, S., R. Taylor, R. B. Smith, and H. Healser (2004a), Changes in geyser eruption behavior and remotely triggered seismicity in Yellowstone National Park produced by the 2002 M 7.9 Denali fault earthquake, Alaska, *Geology*, *32*, 537–540, doi:10.1130/G20381.1.

Husen, S., S. Wiemer, and R. B. Smith (2004b), Remotely triggered seismicity in the Yellowstone National Park region by the 2002 M_w 7.9 Denali fault earthquake, Alaska, *Bull. Seismol. Soc. Am.*, *94*, S317–S331, doi:10.1785/0120040617.

Ide, S., and M. Takeo (1997), Determination of constitutive relations of fault slip based on seismic wave analysis, *J. Geophys. Res.*, *102*(B12), 27,379–27,391.

Johnson, P. A., and X. Jia (2005), Non-linear dynamics, granular media and dynamic earthquake triggering, *Nature*, *437*, 871–874, doi:10.1038/nature04015.

Karner, S. L., and C. Marone (2001), Fractional restrengthening in simulated fault gouge: Effect of shear load perturbations, *J. Geophys. Res.*, *106*(B9), 19,319–19,337.

Kilb, D., J. Gomberg, and P. Bodin (2000), Triggering of earthquake aftershocks by dynamic stresses, *Nature*, *408*, 570–574, doi:10.1038/35046046.

Lockner, D. A., and N. M. Beeler (1999), Premonitory slip and tidal triggering of earthquakes, *J. Geophys. Res.*, *104*(B9), 20,133–20,151, doi:10.1029/1999JB900205.

Mair, K., and C. Marone (1999), Friction of simulated fault gouge for a wide range of velocities and normal stresses, *J. Geophys. Res.*, *104*(B12), 28,899–28,914, doi:10.1029/1999JB900279.

Marone, C. (1998), Laboratory-derived friction laws and their application to seismic faulting, *Annu. Rev. Earth Planet. Sci.*, *26*, 643–696, doi:10.1146/annurev.earth.26.1.643.

Marone, C., and B. Kilgore (1993), Scaling of the critical slip distance for seismic faulting with shear strain in fault zones, *Nature*, *362*, 618–621, doi:10.1038/362618a0.

Marone, C., and C. Scholz (1988), The depth of seismogenic faulting and the upper transition from stable to unstable slip regimes, *Geophys. Res. Lett.*, *15*, 621–624, doi:10.1029/GL015i006p00621.

Prejean, S. G., D. P. Hill, E. E. Brodsky, S. E. Hough, M. J. S. Johnston, S. D. Malone, D. H. Oppenheimer, A. M. Pitt, and K. B. Richards-Dinger (2004), Remotely triggered seismicity on the United States West Coast following the Mw 7.9 Denali fault earthquake, *Bull. Seismol. Soc. Am.*, *94*, S348–S359, doi:10.1785/0120040610.

Rabinowicz, E. (1951), The nature of static and kinetic coefficients of friction, *J. Appl. Phys.*, *22*, 1373–1379, doi:10.1063/1.1699869.

Richardson, E., and T. H. Jordan (2002), Seismicity in deep gold mines of South Africa: Implication for tectonic earthquakes, *Bull. Seismol. Soc. Am.*, *92*, 1766–1782, doi:10.1785/0120000226.

Richardson, E., and C. Marone (1999), Effects of normal stress vibrations on frictional healing, *J. Geophys. Res.*, *104*(B12), 28,859–28,878, doi:10.1029/1999JB900320.

Ruina, A. (1983), Slip instability and state variable friction laws, *J. Geophys. Res.*, *88*(B12), 10,359–10,370.

Savage, H. M., and C. Marone (2007), Effects of shear velocity oscillations on stick-slip behavior in laboratory experiments, *J. Geophys. Res.*, *112*, B02301, doi:10.1029/2005JB004238.

Scholz, C. (1988), The critical slip distance for seismic faulting, *Nature*, *336*, 761–763, doi:10.1038/336761a0.

Scholz, C. (2003), News and views: Good tidings, *Nature*, *425*, 670–671, doi:10.1038/425670a.

Stein, R. (1999), The role of stress transfer in earthquake occurrence, *Nature*, *402*, 605–609, doi:10.1038/45144.

West, M., J. J. Sanchez, and S. R. McNutt (2005), Periodically triggered seismicity at Mount Wrangell, Alaska, after the Sumatra earthquake, *Science*, *308*, 1144–1146, doi:10.1126/science.1112462.

Wong, T.-F., and Y. Zhao (1990), Effects of load point velocity on frictional instability behavior, *Tectonophysics*, *175*, 177–195, doi:10.1016/0040-1951(90)90137-W.

C. Marone, Rock Mechanics Laboratory, Department of Geosciences, Pennsylvania State University, University Park, PA 16802, USA. (cjm@geosc.psu.edu)

H. M. Savage, Department of Earth and Planetary Sciences, Earth and Marine Science, University of California, Santa Cruz, CA 95064, USA. (hsavage@pmc.ucsc.edu)